Performance Analysis of NOMA aided Cooperative Relaying over α-η-κ-μ Fading Channels

Brijesh Soni*, Dhaval K. Patel†, Yong Liang Guan‡, Sumei Sun§, Yoong Choon Chang¶, Joanne Mun-Yee Lim‖
*†School of Engineering and Applied Science, Ahmedabad University, India
‡School of Electrical and Electronic Engineering, Nanyang Technological University, Singapore
§ Institute for Infocomm Research, Singapore
¶ Department of Electrical and Electronic Engineering, Universiti Tunku Abdul Rahman, Malaysia
‖School of Engineering, Monash University, Malaysia
Email: *†{brijesh.soni, dhaval.patel}@ahduni.edu.in, ‡eylguan@ntu.edu.sg, §sunsm@i2r.a-star.edu.sg,
¶ycchang@utar.edu.my, ‖Joanne.Lim@monash.edu

***Abstract*—In this paper, we investigate the outage analysis of Millimeter wave (mmWave) non-orthogonal multiple access (NOMA) based cooperative relaying system. We consider that the source communicates with user equipment with the aid of decode and forward relay using power domain downlink NOMA, and by sending messages in two time slots. Moreover, the α-η-κ-μ fading channel is considered between source, relay and user equipment, which is recently proposed in literature as a good fit model for mmWave communication. To this end, we derive the analytical expression for outage probability in terms of channel fading parameters. In order to gain insights at high SNR, asymptotic analysis for outage probability is carried out. Furthermore, analysis of achievable sum rate is also studied. Findings suggest that the considered channel model provides comparative diversity gain than the other fading channels. Proposed analytical expressions are verified by Monte Carlo simulations. We observe that at high SNR, diversity order depends only on the number of the scattered clusters and on the non linearity of the medium i.e. diversity order is $\alpha\mu/2$.**

***Index Terms*—α-η-κ-μ fading channel, mmWave, NOMA, outage probability, relaying**

I. Introduction

With the growing trend of wireless connected devices and their demanding requirement of high data rate, seamless connectivity, low latency and high capacity, millimeter wave (mmWave) communication has emerged as a potential candidate for 5G. However, one of the challenge of mmWave is its sensitivity to blockage and obstacles. Thus relaying and cooperation among the users are some of the existing solutions to overcome such shortcomings. Moreover, in order to improve the spectral efficiency and maintain user fairness, non-orthogonal multiple access (NOMA) has achieved a great attention in recent years due to its ability to serve multiple devices using same frequency and time resources [1].

There are many works in the literature, which has studied the performance analysis of mmWave NOMA networks under different scenarios. The authors in [2] studied the mmwave NOMA for Internet of Things (IoT) over Rayleigh fading channels. In [3], authors carried out the performance analysis of massive-multiple input multiple output (MIMO) mmwave NOMA over Rayleigh fading channel. Moreover, authors in [4] studied the line of sight and non-line of sight links with different Nakagami-m fading parameters.

In order to exploit the spatial degrees of freedom and to enhance the spatial coverage, research owing to cooperative NOMA has received a significant attention in the recent past. Moreover, cooperative relaying alongwith NOMA improves the throughput of fifth generation wireless networks [5]. Analysis of outage probability in a cooperative NOMA relay selection over Rayleigh fading channel was studied in [6], while the authors in [7] carried out threshold based cooperative NOMA. Authors in [8] derived the capacity analysis of cooperative relaying NOMA over Rayleigh fading channel. The work in [8] was extended by [9], which analysed the cooperative relaying over Rician fading channels. Moreover, authors in [10] focused over $\alpha-\mu$ fading channel while [11] studied over Hoyt fading channel. In addition, authors in [12] carried out the analysis of cooperative NOMA with coordinated direct and relay transmission. All of the aforementioned works have considered the channel models which does not fit well for fifth generation wireless network scenarios.

The recent works in [13], [14] have found that the well established channel models like Rayleigh, Nakagami, Weibull, $\alpha-\mu$, $\kappa-\mu$, etc., does not follow the experimental data for fifth generation communication scenarios like indoor to outdoor propagation, mobile to mobile communication satisfactorily. In [14], a new fading channel model has been proposed namely α-η-κ-μ fading model which encompasses all the traditional and well established channel models. Moreover, this proposed fading model has been verified experimentally in the scenarios like vehicle to vehicle communication, high frequency communications, mobile to mobile propagation, indoor to outdoor propagation in 5G, millimeter communications etc., in [14] and references therein.

The α-η-κ-μ fading model, being in its infant stage, has received a very limited attention. For instance, the capacity analysis of α-η-κ-μ fading channel was investigated in [15], the method of generating samples of α-η-κ-μ channel was studied in [16]. Furthermore, the recent work in [17] carried the bit error rate and outage analysis of α-η-κ-μ fading channel. To the best of the authors' knowledge, no work has been reported in the literature considering the mmWave NOMA based cooperative relaying scheme over the α-η-κ-μ fading channel model for a mobile user, which is a good fit for mmWave communication. The contribution of this work can be summarized as:

- Firstly, we derive the analytical expression for outage probability of transmitted message symbols in two time slots over the α-η-κ-μ fading channel. The derived expressions are validated by Monte Carlo simulations.

- Secondly, in order to gain insight of the system at high SNR the asymptotic analysis for the outage probability is carried out. We posit that the diversity order obtained at high SNR equals $\alpha\mu/2$ indicating that the diversity order depends on the number of multipath clusters and on the non-linearity of the medium.
- Thirdly, we derive the analytical expression for the sum rate analysis for the cooperative relaying scheme. Result indicates the improvement in the achievable sum rate over OMA.

The rest of the paper is organized as follows. Section II describes the preliminaries of α-η-κ-μ fading channel and the considered system model. In Section III we present the performance analysis of outage probability. Section IV focuses on sum rate analysis. Numerical results are discussed in Section V. Finally, Section VI concludes the paper.

II. System and Channel Models

A. Preliminaries of α-η-κ-μ fading channel

The α-η-κ-μ is one of the most generalized and best suited empirical channel model for mmWave communication, vehicle to vehicle communications, indoor-outdoor propagation models in 5G and so on [14]. This fading models takes into account the effect of multipath signals, arbitrary number of dominant components, multipath clustering and non linearity of the medium [15]. The probability density function (PDF) of the envelope of α-η-κ-μ channel is given as [14]

$$f_E(x) = \frac{\alpha x^{\alpha\mu-1} e^{-\left(\frac{x^\alpha}{2}\right)}}{2^\mu \Gamma(\mu)} \sum_{k=0}^{\infty} \frac{k! c_k}{(\mu)_k} L_k^{\mu-1}(2x^\alpha), \qquad (1)$$

where E denotes envelope, c_k is computed with the recursive equation defined in [14, Eq. (15)] where p is the fraction of number of multipath clusters of in-phase and quadrature signals, and q gives the ratio of the power of the dominant components to the power of the scattered waves of the in-phase signal and its counterpart for the quadrature.

The cumulative distribution function (CDF) of the envelope is given by [14]

$$F_E(x) = \frac{x^{\alpha\mu} e^{-\left(\frac{x^\alpha}{2}\right)}}{2^{\mu+1}\Gamma(\mu+1)} \sum_{k=0}^{\infty} \frac{k! m_k}{(\mu+1)_k} L_k^\mu \left(\frac{2(\mu+1)x^\alpha}{\mu}\right), \qquad (2)$$

where m_k is computed using parameters α, η, κ, μ, p, q and with the aid of recursive equation provided in [14, Eq. (16)].

B. System Model

The system model considered in this paper is as shown in Fig. 1. Table I shows the list of mathematical notations used in this paper. We assume downlink mmWave NOMA based cooperative relaying system consisting of high-powered macro base station (S), user equipment (D) and a relay (R) with decode and forward protocol. We consider that the base station consists of a single large antenna which have narrow half-power beamwidth to overcome the pathloss in mmWave communication. Furthermore, we assume that SD link is weaker as compared to SR link. Thus, relay is used in decode and forward mode to transmit message to D. We also assume that relay node has a constant source of power supply. Moreover, D and E operates in a half-duplex mode and are

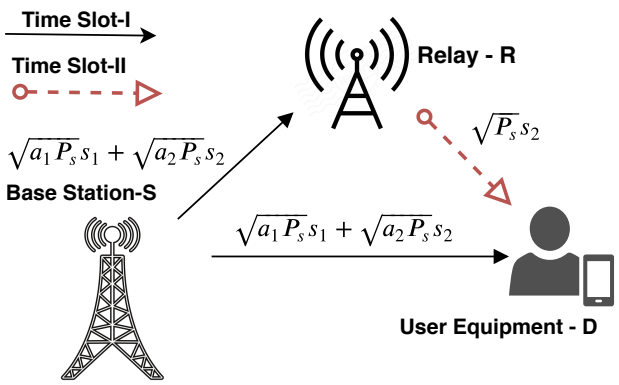

Fig. 1: System model

TABLE I: List of the Notations used

Notation	Description
α	Non-linearity parameter of the medium
η	Ratio of the total power of the in-phase and quadrature scattered waves of multipath clusters
κ	Ratio of total power of dominant components to the scattered total power
μ	Total number of scattered clusters
a_0	Antenna gain
τ	Path loss exponent
d_{SR} , d_{RD} and d_{SD}	Distance between BS to relay, relay to user equipment and BS to user equipment respectively
γ	Instantaneous SINR
ρ	Transmission SNR
λ	$\lvert h\rvert^2$; h is the channel link
$\Gamma(.)$	Gamma function [18, Eq. (8.310.1)]
$(\cdot)_k$	Pochhammer symbol [18, Eq. (6.1.22)]
$L_k^m(.)$	Laguerre polynomial [18, Eq. (8.970.1)]
$G[\,]$	Meijer's G-function
$H[\,]$	Generalized bivariate Fox H function [19]

assumed to be equipped with single antenna. We consider that all the wireless links follow α-η-κ-μ frequency flat fading distribution. Denote the channel fading coefficient between SD, SR, and RD as h_{SD}, h_{SR} and h_{RD} respectively. As per the considered system model, the message transmission occurs in two time slots as follows:

1) Time slot-I: In time slot-I, S broadcasts messages to D and R. Consider the message symbols s_1 and s_2 to be transmitted, multiplexed in power domain. Suppose P_S is transmission power of S and a_1, a_2 are power allocation coefficients with $a_1 + a_2 = 1$ as per NOMA principle and $a_1 > a_2$. Thus, superimposed message can be written as $\mathcal{S} = \sqrt{a_1 P_S}s_1 + \sqrt{a_2 P_S}s_2$.

The signals received at R and D in the first time slot can be written as [2]

$$y_{SR}^1 = \frac{h_{SR}\sqrt{a_0}}{\sqrt{1+d_{SR}^\tau}}(\sqrt{a_1 P_S}s_1 + \sqrt{a_2 P_S}s_2) + n_R,$$

$$y_{SD}^1 = \frac{h_{SD}\sqrt{a_0}}{\sqrt{1+d_{SD}^\tau}}(\sqrt{a_1 P_S}s_1 + \sqrt{a_2 P_S}s_2) + n_D,$$

where n_R and n_D is the complex additive white Gaussian noise with $CN(0,\sigma^2)$. As S sends a superimposed message, relay

$$Pr(O_1) = \frac{w^{0.5\alpha\mu} e^{-\left(\frac{w^{0.5\alpha}}{2}\right)}}{2^{\mu+1}\Gamma(\mu+1)} \sum_{k_1=0}^{\infty} \frac{k_1! m_{k_1}}{(\mu+1)_{k_1}} L_{k_1}^{\mu}\left(\frac{2(\mu+1)w^{0.5\alpha}}{\mu}\right) + \frac{v^{0.5\alpha\mu} e^{-\left(\frac{v^{0.5\alpha}}{2}\right)}}{2^{\mu+1}\Gamma(\mu+1)} \sum_{k_2=0}^{\infty} \frac{k_2! m_{k_2}}{(\mu+1)_{k_2}} L_{k_2}^{\mu}\left(\frac{2(\mu+1)v^{0.5\alpha}}{\mu}\right)$$
$$- \left[\frac{w^{0.5\alpha\mu} e^{-\left(\frac{w^{0.5\alpha}}{2}\right)}}{2^{\mu+1}\Gamma(\mu+1)} \sum_{k_1=0}^{\infty} \frac{k_1! m_{k_1}}{(\mu+1)_{k_1}} L_{k_1}^{\mu}\left(\frac{2(\mu+1)w^{0.5\alpha}}{\mu}\right) \times \frac{v^{0.5\alpha\mu} e^{-\left(\frac{v^{0.5\alpha}}{2}\right)}}{2^{\mu+1}\Gamma(\mu+1)} \sum_{k_2=0}^{\infty} \frac{k_2! m_{k_2}}{(\mu+1)_{k_2}} L_{k_2}^{\mu}\left(\frac{2(\mu+1)v^{0.5\alpha}}{\mu}\right)\right] \quad (9)$$

$$Pr(O_2) = \begin{cases} Pr(\lambda_{SR} < \phi_1) + Pr(\lambda_{SR} \geq \phi_1, \lambda_{SR} < \phi_2) + Pr(\lambda_{SR} > \phi_2, \lambda_{RD} < \frac{\eta_2}{\rho}); & \text{if} \phi_1 < \phi_2 \\ Pr(\lambda_{SR} < \phi_1) + Pr(\lambda_{SR} > \phi_1, \lambda_{RD} < \frac{\eta_2}{\rho}) & \text{Otherwise} \end{cases} \quad (11)$$

$$Pr(O_2) = \frac{\phi_{max}^{0.5\alpha\mu} e^{-\left(\frac{\phi_{max}^{0.5\alpha}}{2}\right)}}{2^{\mu+1}\Gamma(\mu+1)} \sum_{k_1=0}^{\infty} \frac{k_1! m_{k_1}}{(\mu+1)_{k_1}} L_{k_1}^{\mu}\left(\frac{2(\mu+1)\phi_{max}^{0.5\alpha}}{\mu}\right) + \frac{j^{0.5\alpha\mu} e^{-\left(\frac{j^{0.5\alpha}}{2}\right)}}{2^{\mu+1}\Gamma(\mu+1)} \sum_{k_2=0}^{\infty} \frac{k_2! m_{k_2}}{(\mu+1)_{k_2}} L_{k_2}^{\mu}\left(\frac{2(\mu+1)j^{0.5\alpha}}{\mu}\right)$$
$$- \left[\frac{\phi_{max}^{0.5\alpha\mu} e^{-\left(\frac{\phi_{max}^{0.5\alpha}}{2}\right)}}{2^{\mu+1}\Gamma(\mu+1)} \sum_{k_1=0}^{\infty} \frac{k_1! m_{k_1}}{(\mu+1)_{k_1}} L_{k_1}^{\mu}\left(\frac{2(\mu+1)\phi_{max}^{0.5\alpha}}{\mu}\right) \times \frac{j^{0.5\alpha\mu} e^{-\left(\frac{j^{0.5\alpha}}{2}\right)}}{2^{\mu+1}\Gamma(\mu+1)} \sum_{k_2=0}^{\infty} \frac{k_2! m_{k_2}}{(\mu+1)_{k_2}} L_{k_2}^{\mu}\left(\frac{2(\mu+1)j^{0.5\alpha}}{\mu}\right)\right] \quad (12)$$

has to decode s_1 out of it. Instantaneous SINR at relay in time slot-I while decoding message s_1 can be written as:

$$\gamma_{SR}^{s_1} = \frac{a_1\rho\lambda_{SR}}{a_2\rho\lambda_{SR} + d_{SR}^{\tau}}, \quad (3)$$

Successive interference cancellation (SIC) is performed to remove s_1 from superimposed signal. The instantaneous SNR for decoding s_2 can be written as:

$$\gamma_{SR}^{s_2} = \frac{a_2\rho\lambda_{SR}}{d_{SR}^{\tau}}. \quad (4)$$

In similar fashion, the SINR at D, for decoding symbol s_1 can be computed as:

$$\gamma_{SD}^{s_1} = \frac{a_1\rho\lambda_{SD}}{a_2\rho\lambda_{SD} + d_{SD}^{\tau}}. \quad (5)$$

2) Time slot-II: In time slot-II, Relay sends $\hat{s_2}$, the estimated s_2 to D with power P_R. So, at D, the received signal can be written as

$$y_{RD}^{s_2} = \frac{h_{RD}\sqrt{a_0}}{\sqrt{1+d_{RD}^{\tau}}}(\sqrt{a_2 P_R}\hat{s_2}) + n_D. \quad (6)$$

The instantaneous SNR at the D, for decoding s_2, is given by

$$\gamma_{RD}^{s_2} = \frac{\lambda_{RD}\rho}{d_{RD}^{\tau}} \quad (7)$$

Thus in the considered relaying scheme, two symbols will be delivered to the destination in the two time slots as opposed to the OMA based cooperative relaying wherein only one symbol will be delivered in two time slots.

III. Performance Analysis of Outage Probability

The comprehensive analysis for outage probability of s_1 and s_2 is carried out in this section. The outage probability is defines as the probability of the event wherein certain quantities or physical measurements cannot meet the predefined threshold.

A. Outage Probability of s_1

The data rates of symbols s_1, s_2 and are given as R_1, R_2 respectively. The outage for message symbol s_1 can be defined as the event where either the relay R or the D fails to decode s_1 successfully. Therefore, the outage probability of symbol s_1 for a given target data rate R_1 can be written as

$$\begin{aligned} Pr(O_1) &= Pr(C_{S1} < R_1) \\ &= 1 - Pr[min(\gamma_{SR}, \gamma_{SD}) > \phi_1] \\ &= 1 - Pr[\gamma_{SR} > \phi_1] Pr[\gamma_{SD} > d_1] \\ &= F_{\lambda_{SR}}(\phi_1) + F_{\lambda_{SD}}(\phi_1^{'}) - F_{\lambda_{SR}}(\phi_1) F_{\lambda_{SD}}(\phi_1^{'}), \end{aligned} \quad (8)$$

where $Pr(O_1)$ is the event representing s_1 in outage, $\eta_1 = 2^{2R_1} - 1$ and $\phi_1 = \frac{\eta_1}{\rho(a_1 - \eta_1 a_2)}$. It must be noted that $a_1 > \eta_1 a_2$, otherwise the outage of s_1 will always occur. On substituting ϕ_1 in (8), the expression for $Pr(O_1)$ is obtained in (9).

For proof, refer to Appendix A and Appendix B ■

B. Outage probability of s_2

In this section we compute the outage probability of symbol s_2, denoted by O_2. The outage depends on the three events as: $O_2 = E_1 \cup E_2 \cup E_3$, where E_1 indicates the event when the relay cannot successfully decoded s_1, E_2 is the event when relay successfully decodes s_1, but fails to decode symbol s_2 and E_3 is the event when both s_1 and s_2 are successfully decoded at the relay, but the destination fails to decode symbol s_2. Moreover, the events E_1, E_2 and E_3 are disjoint. For target data rate R_2, the outage probability of the symbol can be written as (10) and (11)

$$Pr(O_2) = F_{\lambda_{SR}}(\phi_{max}) + F_{\lambda_{RD}}(j) - F_{\lambda_{SR}}(\phi_{max}) F_{\lambda_{RD}}(j), \quad (10)$$

where $\eta_2 = 2^{2R_2} - 1$, $\phi_2 = \frac{\eta_2}{a_2\rho}$, $j = \frac{\eta_2}{\rho}$ and $\phi_{max} = max\{\phi_1, \phi_2\}$. On further solving, the expression in (11) can be re-written as (12).

C. Asymptotic analysis of s_1 and s_2

To gain more insights at high SNR, we carry out the asymptotic analysis in this section. For sake of clarity, we rewrite the CDF of SNR as:

$$F_\lambda(\phi_1)=\frac{\sqrt{\phi_1}^{\alpha\mu}e^{-\left(\frac{\sqrt{\phi_1}^{\alpha}}{2}\right)}}{2^{\mu+1}\Gamma(\mu+1)}\sum_{k=0}^{\infty}\frac{k!m_k}{(\mu+1)_k}L_k^{\mu}\left(\frac{2(\mu+1)\sqrt{\phi_1}^{\alpha}}{\mu}\right).$$

On using the definition of Pochhammer symbol and on series expansion of exponential and L_k^{μ}, we obtain

$$F_\lambda(\phi_1)=\frac{\sqrt{\phi_1}^{\alpha\mu}}{2^{\mu+1}\Gamma(\mu+k+1)}\sum_{k=0}^{\infty}\sum_{l=0}^{\infty}\sum_{z=0}^{k}\frac{k!m_k(-1)^{l+z}}{l!}\times L_k^{\mu}\left(\frac{2(\mu+1)\sqrt{\phi_1}^{\alpha}}{\mu}\right)\times\binom{k+\mu}{k-z}\times\frac{1}{z!}\left(\frac{2(\mu+1)\sqrt{\phi_1}^{\alpha}}{\mu}\right)^{z} \tag{13}$$

On replacing ϕ_1 with $\frac{\eta_1 d_{SD}^{\tau}}{\rho(a_1-\eta_1 a_2)}$, and on further simplification, we obtain

$$F_\lambda(\phi_1)=\frac{\rho^{-\frac{\alpha\mu}{2}}}{2^{\mu+1}\Gamma(\mu+k+1)}\left(\frac{\eta_1 d_{SD}^{\tau}}{a_1-\eta_1 a_2}\right)^{\frac{\alpha\mu}{2}}\sum_{k=0}^{\infty}\sum_{l=0}^{\infty}\sum_{z=0}^{k}\frac{k!m_k(-1)^{l+z}}{l!}\times\frac{\rho^{\frac{-\alpha z}{2}}}{2z!}\times\binom{k+\mu}{k-z}\times\left(\frac{\eta_1 d_{SD}^{\tau}}{a_1-\eta_1 a_2}\right)^{\frac{\alpha l+\alpha z}{2}} \tag{14}$$

From above expression, we can conclude that at high SNR $F_\lambda(\phi_1)$ depends only on the fading parameters α and μ i.e., it depends on non linearity parameter of the medium and on the number of scattered clusters. The diversity order of s_1 as observed from the above expression is $\frac{\alpha\mu}{2}$. The diversity order of s_2 can be computed in similar way as s_1.

IV. Sum rate analysis

The symbol s_1 should be decoded at the relay for SIC and at the destination as well. The achievable rate for symbol s_1 can be written as

$$\begin{aligned}C_{s_1}&=0.5\min\left\{\log_2(1+\gamma_{SD}),\log_2\left(1+\gamma_{SR}^{I}\right)\right\}\\&=0.5\log_2\left(1+\frac{X\rho a_1}{X\rho a_2+1}\right)\\&=0.5\log_2(1+X\rho)-0.5\log_2(1+X\rho a_2).\end{aligned}$$

Similarly, the achievable rate for symbol s_2 can be given as

$$\begin{aligned}C_{s_2}&=0.5\min\{\log_2(1+\gamma_{SR}),\log_2(1+\gamma_{RD})\}\\&=0.5\log_2(1+\min\{\lambda_{SR}\rho a_2,\lambda_{RD}\rho\})=0.5\log_2(1+\rho Y),\end{aligned}$$

where $X\triangleq\min\{\lambda_{SD},\lambda_{SR}\}$ and $Y\triangleq\min\{\lambda_{SR}\rho a_2,\lambda_{RD}\}$. Therefore, the average achievable rate for s_1 can be written as

$$\bar{C}_{s_1}=\frac{0.5}{\ln(2)}\left[\underbrace{\int_0^{\infty}\ln(1+\rho x)f_X(x)dx}_{\varpi_1}-\underbrace{\int_0^{\infty}\ln(1+a_2\rho x)f_X(x)dx}_{\varpi_2}\right] \tag{15}$$

On utilizing the PDF[1], the expression for ϖ_1 can be simplified as

$$\varpi_1=\underbrace{\int_0^{\infty}\ln(1+\rho x)f_{\lambda_{sr}}(x)dx}_{I_1}-\underbrace{\int_0^{\infty}\ln(1+\rho x)f_{\lambda_{sr}}(x)F_{\lambda_{sd}}(x)\,dx}_{I_2}+\underbrace{\int_0^{\infty}\ln(1+\rho x)f_{\lambda_{sd}}(x)dx}_{I_3}-\underbrace{\int_0^{\infty}\ln(1+\rho x)f_{\lambda_{sd}}(x)F_{\lambda_{sr}}(x)\,dx}_{I_4}$$

[1]The pdf of X can be given as $f_X(x)=f_{\lambda_{sr}}(x)-f_{\lambda_{sr}}(x)F_{\lambda_{sd}}(x)+f_{\lambda_{sd}}(x)-f_{\lambda_{sd}}(x)F_{\lambda_{sr}}(x)$.

On substituting the value of PDF of instantaneous SNR from [20] and on further simplification, I_1 can be expressed as

$$I_1=\frac{\alpha}{2^{\mu}\rho^{\frac{\alpha\mu}{2}}}\sum_{k=0}^{\infty}\sum_{z=0}^{k}\frac{(-1)^z}{z!}\binom{k+\mu-1}{k-m}\frac{k!c_k}{\Gamma(\mu+k)\rho^{\frac{\alpha\mu}{2}}}\times\int_0^{\infty}x^{(\frac{\alpha\mu+\alpha m}{2})-1}\exp\left(\frac{-x^{\frac{\alpha}{2}}}{2\rho^{\frac{\alpha}{2}}}\right)\ln(1+\rho x)dx. \tag{16}$$

On expressing the exponential and logarithmic functions in terms of Meijer's G-functions [21] gives

$$I_1=\frac{\alpha}{2^{\mu}\rho^{\frac{\alpha\mu}{2}}}\sum_{k=0}^{\infty}\sum_{z=0}^{k}\frac{(-1)^z}{z!}\binom{k+\mu-1}{k-m}\frac{k!c_k}{\Gamma(\mu+k)\rho^{\frac{\alpha\mu}{2}}}\times\int_0^{\infty}x^{(\frac{\alpha\mu+\alpha m}{2})-1}\times G_{0,1}^{1,0}\left(\frac{-x^{\frac{\alpha}{2}}}{2\rho^{\frac{\alpha}{2}}}\Big|_0^{-}\right)G_{2,2}^{1,2}\left(\rho x\Big|_{1,0}^{1,1}\right)dx. \tag{17}$$

On utilizing the identity from [21, eqn.(7),(21)], the above expression can be written as

$$I_1=\frac{\alpha_{sr}}{2_{sr}^{\mu}\rho^{\frac{\alpha_{sr}\mu_{sr}}{2}}}\sum_{k=0}^{\infty}\sum_{z=0}^{k}\frac{(-1)^z}{z!}\binom{k+\mu-1}{k-m}\frac{k!c_k\rho^{\bar{\alpha}}}{\Gamma(\mu+k)\rho^{\frac{\alpha\mu}{2}}(2\pi)^{\alpha_{sr}-0.5}}\times G_{2\alpha_{sr},2+2\alpha_{sr}}^{2+2\alpha_{sr},\alpha_{sr}}\left(\frac{0.5\rho^{-\alpha_{sr}}\cdot 2^{-2}}{\rho_{sr}^{\alpha}}\Big|_{\Delta(2,0),\Delta(\alpha,1-\bar{\alpha}),\Delta(\alpha,1-\bar{\alpha})}^{\Delta(2,-\bar{\alpha}),\Delta(2,1-\bar{\alpha})}\right), \tag{18}$$

where $\bar{\alpha}=(\frac{\alpha_{sr}\mu_{sr}+\alpha_{sr}m}{2})$. Similarly, on utilizing the definition of CDF and PDF, I_2 can be simplified as

$$I_2=\sum_{k_1=0}^{\infty}\sum_{z_1=0}^{k_1}\frac{\alpha_{sr}}{2^{\mu_{sr}+\mu_{sd}+2}\Gamma(\mu_{sd}+1)\rho^{\frac{\alpha_{sr}\mu_{sr}}{2}}}\frac{(-1)^{z_1}}{z_1!}\binom{k_1+\mu-1}{k_1-z_1}\times\frac{k_1!c_{k_1}2^{z_1}\rho^{-\frac{\alpha_{sr}z_1}{2}}}{\Gamma(\mu_{sr}+k_1)}\sum_{k_2=0}^{\infty}\sum_{z_2=0}^{k_2}\frac{(-1)^{z_2}\cdot 2k_2!}{\mu_{sd}z_2!k_2}\binom{k_2+\mu}{k_2-z_2}m_{k_2}\rho^{-\frac{\alpha_{sd}}{2}}\times\int_0^{\infty}x^{\beta-1}\exp\left(\frac{-x^{\frac{\alpha_{sr}}{2}}}{2\rho^{\frac{\alpha_{sr}}{2}}}\right)\exp\left(\frac{-x^{\frac{\alpha_{sd}}{2}}}{2\rho^{\frac{\alpha_{sd}}{2}}}\right)\ln(1+\rho x)dx, \tag{19}$$

where $\beta=\frac{\alpha_{sr}z_1+\alpha_{sr}\mu_{sr}+\alpha_{sd}\mu_{sd}+\alpha_{sd}}{2}$. On following similar steps as in previous expression, and on replacing with equivalent Meijer's G-function, we obtain

$$I_2=\sum_{k_1=0}^{\infty}\sum_{z_1=0}^{k_1}\frac{\alpha_{sr}}{2^{\mu_{sr}+\mu_{sd}+2}\Gamma(\mu_{sd}+1)\rho^{\frac{\alpha_{sr}\mu_{sr}}{2}}}\frac{(-1)^{z_1}}{z_1!}\binom{k_1+\mu-1}{k_1-z_1}\times\frac{k_1!c_{k_1}2^{z_1}\rho^{-\frac{\alpha_{sr}z_1}{2}}}{\Gamma(\mu_{sr}+k_1)}\sum_{k_2=0}^{\infty}\sum_{z_2=0}^{k_2}\frac{(-1)^{z_2}\cdot 2k_2!}{\mu_{sd}z_2!k_2}\binom{k_2+\mu}{k_2-z_2}m_{k_2}\rho^{-\frac{\alpha_{sd}}{2}}\times\int_0^{\infty}x^{\beta-1}G_{0,1}^{1,0}\left(\frac{-x^{\frac{\alpha_{sr}}{2}}}{2\rho^{\frac{\alpha_{sr}}{2}}}\Big|_0^{-}\right)G_{0,1}^{1,0}\left(\frac{-x^{\frac{\alpha_{sd}}{2}}}{2\rho^{\frac{\alpha_{sd}}{2}}}\Big|_0^{-}\right)G_{2,2}^{1,2}\left(\rho x\Big|_{1,0}^{1,1}\right)dx. \tag{20}$$

Further, on expressing Meijer's G-function into its equivalent Fox H-function, the expression can be simplified as (21) as shown on top of the next page.

In similar way, I_3 can be derived as I_1 and I_4 can be derived as I_2. Moreover, ϖ_2 will also consist of four terms, expressions of which can be obtained by replacing ρ by $a_2\rho$ in I_1-I_4. Also, notice that the expression of $\bar{C}_{s_2}$ is similar to $\bar{C}_{s_1}$. Thus, on transforming the random variables and on solving in similar lines with I_1-I_4, the analytical expression can be derived.

$$I_2 = \sum_{k_1=0}^{\infty}\sum_{z_1=0}^{k_1} \frac{\alpha_{sr}}{2^{\mu_{sr}+\mu_{sd}+2}\Gamma(\mu_{sd}+1)\rho^{\frac{\alpha_{sr}\mu_{sr}}{2}}} \frac{(-1)^{z_1}}{z_1!}\binom{k_1+\mu-1}{k_1-z_1} \times \frac{k_1! c_{k_1} 2^{z_1}\rho^{-\frac{\alpha_{sr}z_1}{2}}}{\Gamma(\mu_{sr}+k_1)} \sum_{k_2=0}^{\infty}\sum_{z_2=0}^{k_2} \frac{(-1)^{z_2}\cdot 2k_2!}{\mu_{sd}z_2!k_2}\binom{k_2+\mu}{k_2-z_2} m_{k_2}\rho^{-\frac{\alpha_{sd}}{2}}$$
$$\times H_{1,0:0,1:2,2}^{0,1:1,0:1,2}\left[\left(1-\beta;\frac{\alpha_{sd}}{\alpha_{sr}},\frac{2}{\alpha_{sr}}\right)\middle|\begin{matrix}-\\(0,1)\end{matrix}\middle|\begin{matrix}(1,1),(1,1)\\(1,1),(0,1)\end{matrix}\middle|\left(\frac{-\rho^{\frac{\alpha_{sd}}{2}}}{2\rho^{\frac{\alpha_{sd}}{2}}}\right),\frac{-\rho^{\frac{\alpha_{sr}}{2}}}{2\rho^{\frac{\alpha_{sr}}{2}}}\right] \quad (21)$$

V. Numerical Results

In this section, we quantify the effect of fading parameters on the outage probability for the considered system model by providing analytical, asymptotic and simulation plots. We assume that the parameters α, η, κ, μ for *SR*, *SD* and *RD* links to be same. For validation of results, we generated the samples as described in [16]. Moreover, the parameter values used are as follows: $\tau = 1.5$, $a_0 = 6$ dB $= 4$, $a_1 = 0.9$, $a_2 = 0.1$ and the predefined threshold $R_1 = 0.5$ and $R_2 = 0.3$ bps/Hz. The values of p and q is 1 and 1.5 respectively, unless otherwise stated. In all figures, solid lines represent analytical plot, dashed lines represent asymptotic plot and markers represent simulation plot. Fig. 2 shows the plot of outage probability of s_1 versus varying transmission SNR for different channel fading parameters. The result is plotted for $d_{SR} = 2$m and $d_{SD} = 4$m. The markers shows the simulation plots, in good agreement with the analytical results while the dashed line indicates the asymptotic plot. As can be noticed from the plot, slope is highest for 60 GHz LOS link and least for the Rayleigh fading channel, and thus α-η-κ-μ fading channel provides the maximum diversity gain. Notice that although (9) contains the sum involving infinite terms, it converges quickly after 15 terms. We can also notice that the considered channel model incorporates all the fading models. Fig. 3 shows the

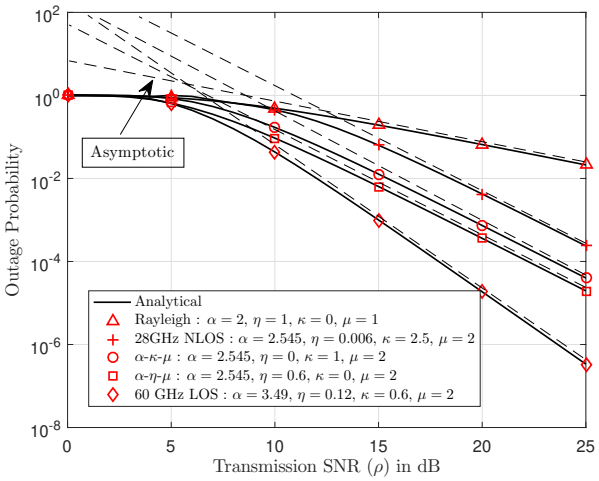

Fig. 2: Outage probability of s_1

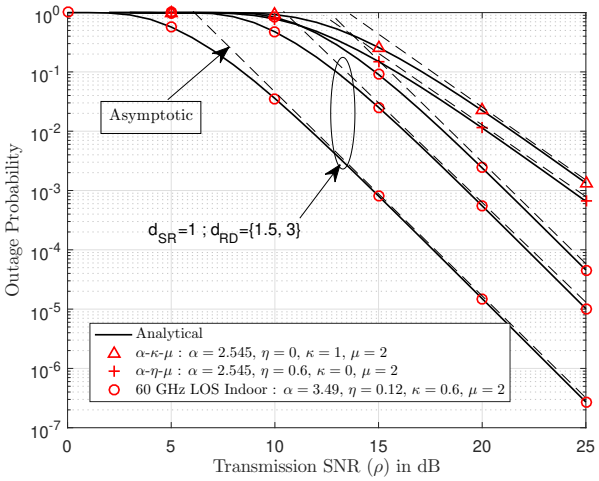

Fig. 3: Outage probability of s_2

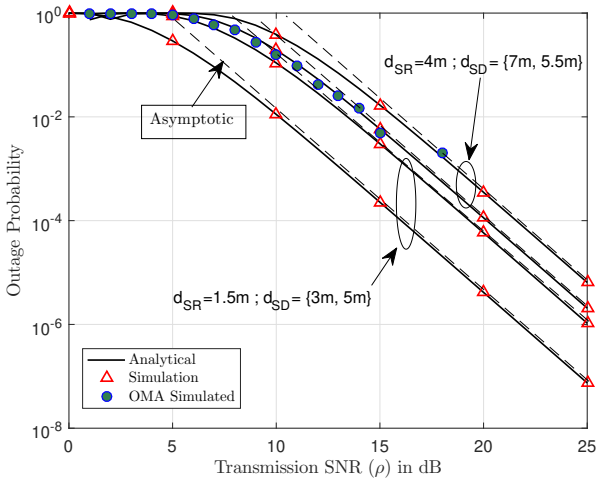

Fig. 4: Effect of distance on the outage probability of s_1

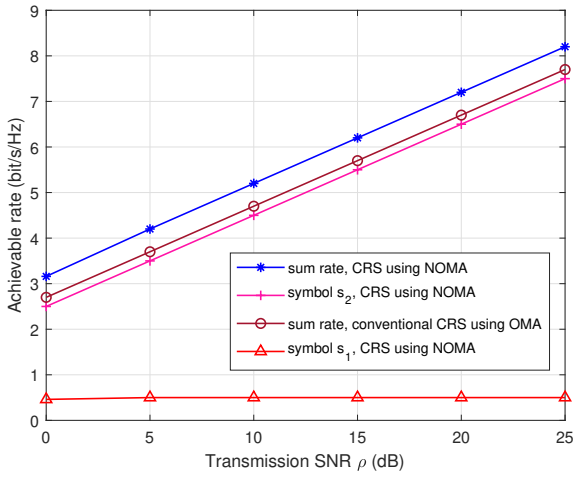

Fig. 5: Achievable sum rate comparison for NOMA and OMA aided cooperative relaying scheme

combined effect of fading parameters and varying distance for the considered system model on the outage probability of s_2. Markers with circle represent 60 GHz LOS indoor link. We can notice that the slope of this link is maximum, thus providing the maximum diversity gain. Moreover, the slopes of all the circle markers are same, thus providing same diversity gain. For comparison of the proposed scheme, we simulated OMA for the considered system model, $d_{SR} = 1.5m$ and $d_{SD} = 3m$. Fig. 4 shows the effect of varying distance on the outage probability of s_1. This result is plotted for 60 GHz LOS indoor communication link with parameters considered from the empirical distribution in [22]. We can notice that as the distance between cooperative users increases, outage increases. By knowing the bearable outage beforehand, this result can help in the positioning of relay devices for mmWave based communications. Fig. 5 indicates the achievable sum rate comparison for NOMA and OMA aided cooperative relaying scheme for $\alpha = 2.545$, $\eta = 0.0006$, $\kappa = 2.5$, $\mu = 2$, $d_{SR} = d_{RD} = 1m$ and $d_{SD} = 2m$. We can observe from the plot that sum rate for cooperative relaying scheme is better for NOMA as compared to OMA. This is expected due to the fact that in NOMA, two symbols are transmitted in two time slots as compared to OMA wherein only one symbol is transmitted.

VI. Conclusions

In this paper, outage probability of a mmWave NOMA based cooperative relaying scheme considering the α-η-κ-μ fading channel is investigated. We derive the expression for the performance analysis of outage probability for two message symbols in two time slots along with the asymptotic analysis to gain insights of the proposed scheme at high SNR. Sum rate analysis of the proposed scheme is also derived. We conclude that the considered fading model provides the highest diversity gain and also encompasses all the well established traditional channel models. In addition, the proposed scheme also outperforms OMA for the considered system model. Furthermore, α-η-κ-μ fading model can be a more realistic consideration for the scenarios including mmwave MIMO NOMA and downlink mmwave NOMA with unordered channels.

Acknowledgment

The authors would like to thank financial support received under the DST ASEAN project (grant ref. IMRC/AISTDF/R&D/P-09/2017). The authors also thank Ahmedabad University for the infrastructural support.

Appendix A
Derivation of ϕ_1 and $\phi_1^{'}$

Let us assume that $\lambda_{SR} = \phi_1$. From (3), we can write

$$\gamma_{SR} a_2 \rho \lambda_{SR} + \gamma_{SR} d_{SR}^{\tau} = a_1 \rho \lambda_{SR}. \tag{22}$$

On arranging the terms, we obtain

$$\phi_1 = \frac{\gamma_{SR} d_{SR}^{\tau}}{a_1 \rho - \gamma_{SR} a_2 \rho} = \frac{\eta_1 d_{SR}^{\tau}}{\rho(a_1 - \eta_1 a_2)} = w. \tag{23}$$

Similarly, let $\lambda_{SD} = \phi_1^{'}$, on solving further we have

$$\phi_1^{'} = \frac{\eta_1 d_{SD}^{\tau}}{\rho(a_1 - \eta_1 a_2)} = v. \tag{24}$$

Appendix B
Derivation of $F_{\lambda b}(x)$

The expression in (2) gives the CDF of the envelope. However, we require the CDF of channel gain $\lambda_b = |h_b|^2$, b = $\{SR, SD, SE\}$ Thus, from the definition of CDF, we have,

$$\begin{aligned} F_{\lambda b}(x) &= \int_0^{\sqrt{x}} f_{\lambda b}(\omega) d\omega \\ &= \frac{\sqrt{x}^{\alpha\mu} e^{-\left(\frac{\sqrt{x}^{\alpha}}{2}\right)}}{2^{\mu+1}\Gamma(\mu+1)} \sum_{k=0}^{\infty} \frac{k! m_k}{(\mu+1)_k} L_k^{\mu}\left(\frac{2(\mu+1)\sqrt{x}^{\alpha}}{\mu}\right). \end{aligned} \tag{25}$$

References

[1] Y. Niu, Y. Li, D. Jin, L. Su, and A. V. Vasilakos, "A survey of millimeter wave communications for 5G: opportunities and challenges," *Wireless netw.*, vol. 21, no. 8, pp. 2657–2676, 2015.

[2] H. Sun, Q. Wang, S. Ahmed, and R. Q. Hu, "Non-orthogonal multiple access in a mmwave based IoT wireless system with SWIPT," in *Proc. of IEEE VTC*, Jun. 2017, pp. 1–5.

[3] Z. Ding, L. Dai, R. Schober, and H. Vincent Poor, "NOMA meets finite resolution analog beamforming in massive MIMO and millimeter-wave networks," *IEEE Commun. Lett.*, vol. 21, no. 8, pp. 1879–1882, Aug. 2017.

[4] Y. Sun, Z. Ding, and X. Dai, "On the performance of downlink NOMA in multi-cell mmwave networks," *IEEE Commun. Lett.*, vol. 22, no. 11, pp. 2366–2369, Nov. 2018.

[5] Y. Liu, Z. Ding, M. Elkashlan, and H. V. Poor, "Cooperative non-orthogonal multiple access with simultaneous wireless information and power transfer," *IEEE J. Sel. Areas Commun.*, vol. 34, no. 4, pp. 938–953, Apr. 2016.

[6] H. Sun, Q. Wang, R. Q. Hu, and Y. Qian, "Outage probability study in a NOMA relay system," in *Proc. of IEEE WCNC*, Mar. 2017, pp. 1–6.

[7] F. Kara and H. Kaya, "Threshold-based selective cooperative-NOMA," *IEEE Commun. Lett.*, vol. 23, no. 7, pp. 1263–1266, Jul. 2019.

[8] J. Kim and I. Lee, "Capacity analysis of cooperative relaying systems using non-orthogonal multiple access," *IEEE Commun. Lett.*, vol. 19, no. 11, pp. 1949–1952, Nov 2015.

[9] R. Jiao, L. Dai, J. Zhang, R. MacKenzie, and M. Hao, "On the performance of NOMA-based cooperative relaying systems over Rician fading channels," *IEEE Trans. Veh. Technol.*, vol. 66, no. 12, pp. 11 409–11 413, Dec. 2017.

[10] V. Kumar, B. Cardiff, and M. F. Flanagan, "Performance analysis of NOMA-based cooperative relaying in $\alpha-\mu$ fading channels," in *Proc. of IEEE ICC*, May 2019, pp. 1–7.

[11] S. R. Panic and D. N. K. Jayakody, "Performance analysis of NOMA-based cooperative relay systems over Hoyt fading channels," in *Proc. of IEEE VTC*, Apr. 2019, pp. 1–5.

[12] M. Yang, J. Chen, L. Yang, L. Lv, B. He, and B. Liu, "Design and performance analysis of cooperative NOMA with coordinated direct and relay transmission," *IEEE Access*, vol. 7, pp. 73 306–73 323, 2019.

[13] Y. Ibdah and Y. Ding, "Mobile-to-mobile channel measurements at 1.85 GHz in suburban environments," *IEEE Trans. Commun.*, vol. 63, no. 2, pp. 466–475, Feb. 2015.

[14] M. D. Yacoub, "The α-η-κ-μ fading model," *IEEE Trans. Antennas Propag.*, vol. 64, no. 8, pp. 3597–3610, Aug. 2016.

[15] X. Li, X. Chen, J. Zhang, Y. Liang, and Y. Liu, "Capacity analysis of α-η-κ-μ fading channels," *IEEE Commun. Lett.*, vol. 21, no. 6, pp. 1449–1452, Jun. 2017.

[16] V. M. Renno, R. A. A. de Souza, and M. Daoud Yacoub, "On the generation of α-η-κ-μ samples with applications," in *Proc. of PIMRC*, Oct. 2017, pp. 1–5.

[17] J. M. Moualeu, D. B. da Costa, F. J. Lopez-Martinez, and R. A. A. d. Souza, "On the performance of α-η-κ-μ fading channels," *IEEE Commun. Lett.*, vol. 23, no. 6, pp. 967–970, Jun. 2019.

[18] D. Zwillinger, *"Table of Integrals, Series, and Products", Eighth Edition*, 2014.

[19] A. M. Mathai, R. K. Saxena, and H. J. Haubold, *The H-function: theory and applications*. Springer Science & Business Media, 2009.

[20] A. Mathur, Y. Ai, M. R. Bhatnagar, M. Cheffena, and T. Ohtsuki, "On physical layer security of α-η-κ-μ fading channels," *IEEE Commun. Lett.*, vol. 22, no. 10, pp. 2168–2171, Oct. 2018.

[21] V. S. Adamchik and O. I. Marichev, "The algorithm for calculating integrals of hypergeometric type functions and its realization in reduce system," in *Proc. of ISSAC*, New York, USA, 1990, pp. 212–224.

[22] A. A. dos Anjos, T. R. R. Marins, R. A. A. de Souza, and M. D. Yacoub, "Higher order statistics for the $\alpha-\eta-\kappa-\mu$ fading model," *IEEE Trans. Antennas Propag.*, vol. 66, no. 6, pp. 3002–3016, Jun. 2018.